Optimal Battery Energy Storage System Sizing for Demand Charge Management in EV Fast Charging Stations

Koolman, George ; Stecca, Marco; Bauer, Pavol

DOI
10.1109/ITEC51675.2021.9490138

Publication date
2021

Document Version
Accepted author manuscript

Published in
2021 IEEE Transportation Electrification Conference & Expo (ITEC)

Optimal Battery Energy Storage System Sizing for Demand Charge Management in EV Fast Charging Stations

George Koolman, Marco Stecca and Pavol Bauer
Dept. of Electrical Sustainable Energy
Delft University of Technology
Delft, Netherlands
georgekoolman@gmail.com
{m.stecca & p.bauer}@tudelft.nl

***Abstract*—The high pulsating demand of fast charging stations (FCS) may cause monthly demand charges to account for a significant fraction of a station's electric bill. To reduce these costs, demand charge management can be applied to suppress peak power demands at FCSs, also using battery energy storage systems (BESS). This paper proposes a multi-objective approach for the optimal BESS and grid-tie sizing in FCS designs using genetic algorithms. With demand data from a FCS in the Netherlands, numerical studies are conducted in the Mosaik and Pymoo environments to assess the effectiveness of the proposed formulation.**

***Index Terms*—battery energy storage systems, demand charge management, electrical vehicles, fast charging stations, genetic algorithms, multi-objective optimizations, NSGA-II**

I. Introduction

The transportation sector accounts for approximately 25% of the global energy-related emissions. Of these emissions, around 70% is due to the use of combustion vehicles [1]. One of the major disruptions to the transportation sector, set to tackle our carbon emission problem, is the wide adoption of electrical vehicles (EV). However, concerns related to charging speeds and driving range continue to be wide spread among consumers. A study has shown that 83% of consumers who would not consider an EV, cites 'range anxiety' or 'charging anxiety' as the reason [2].

ElaadNl, a Dutch research center in the field of EVs, list location issues and demand charges as the two major concerns related to installing fast charging stations (FCSs) [3]. Demand charge is a fee based on the highest measured peak power (in kW) during a monthly billing period. The demand tariff is the price per kW the DSO uses to determine these monthly fees and can vary significantly between regions, e.g. the Netherlands (€3/kW) and New York ($50/kW) [4]. These demand charges can therefore account for a significant portion (up to 90%) of a FCSs electric bill, consequently weakening the business case for a FCS [5]. Under such circumstances there is a clear incentive for FCS owners to limit their peak power usage by implementing battery energy storage systems (BESS) assisted demand charge management (DCM) at their stations [4].

From the literature it is clear that BESS is a feasible solution for reducing the peak power demands and demand charges at FCSs [6]–[11]. However, the literature contains mostly research on sizing optimizations based on one objective, either costs or waiting times. Whereas research into multi-objective optimizations investigating how both objectives impact the BESS sizing and limited grid-tie ratings is lacking. These aspects are important to FCS owners due to the large investments of BESS projects and the limited trade-off on waiting times (quality of service) at FCSs. This paper proposes a multi-objective optimization (MOO) framework using NSGA-II for the optimal BESS and grid-tie sizing at FCSs in order to reduce demand charges and charging delays.

The remainder of this paper is structured as follows. In Section II the BESS assisted FCS modeling approach is presented. The multi-objective problem is formulated and the proposed sizing framework is presented in Section III. Section IV describes the case studies and the optimization, and the numerical simulation results are presented in Section V. Lastly, the paper is concluded in Section VI.

II. FCS Modeling

In general this model simulates the power flows inside a BESS assisted AC configuration FCS that includes, a N number of DC fast charging stalls, a lithium iron phosphate (LFP/C) BESS and grid-tie that couples the station to the MV grid. An AC configuration is selected due to it's maturity and standard of application at most FCS [12], and a LFP/C BESS due to it's high suitability for grid-connected applications [13]. Furthermore, the task intended for the BESS is to perform peak-shaving on the demand in order to restrict the grid-tie power to a set limit, and thus reducing the stations demand charges.

The model inputs are based on the following design parameters, BESS capacity in kWh, BESS power rating in kW, maximum grid-tie power in kW and a minute resolution

This research was done in collaboration with Royal HaskoningDHV and the paper submission was funded by Stichting 3E.

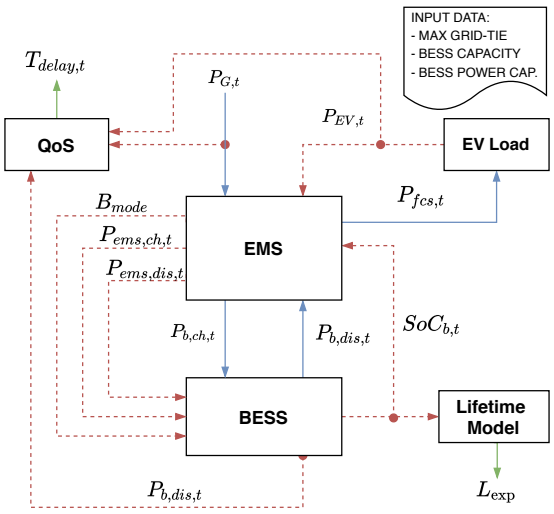

Fig. 1: System diagram of the complete simulation model

demand profile of a FCS. The outputs for this model are given in the following performance parameters, BESS SOC in %, the power flows in kW, charging delays in minutes and the expected BESS lifetime in years. An important assumption made regarding the charging delays, is that when both the restricted grid-tie and BESS reach their designed power limits, it is assumed that a simple power balancing technique is being employed by the charging stalls. This results in equally divided charging delays among active stalls.
Fig. 1 depicts the corresponding inter-connection and data exchange between the five modules included in this model, the EV demand, energy management system (EMS), BESS, lifetime model and quality of service (QoS). The blue lines represent the physical power flows, the red dotted lines the signal exchange between each modules and the green lines the performance related results. During the simulation only the red signals are exchanged between modules and the blue and green lines are represented as output results from these modules. This complete model is implemented using the python based Mosaik smart-grid simulation environment [14].

Charging sessions at FCS typically range from 10-30 minutes, can vary per EV model and does not have a constant power during the entire charging duration [15]. Additionally, the maximum permissible charging delays can be estimated between 0-6 minutes [6]. Hence, a model resolution (simulation step t) of one minute is selected to ensure capture of the session scale charging characteristics in the FCS demand profile and help give a close approximation of the charging delays. It should be noted however, that due to the post-processing nature of the BESS lifetime model, this parameter is calculated at the end of each simulation.

A. Station Demand

The module "EV demand" models the total power demand of all EVs charging at the FCS. For each simulation interval t, this module generates the EV power demand $P_{EV,t}$ in kW for a defined station. For this a pre-defined minute scale power demand profile of a FCS is required for the initialization. These profiles can either be estimated from stochastic models or obtained from measurement data.

B. Energy Management System

In this model the EMS is regarded as the central unit of the system. This model performs the correct power flow controls for the FCS in order to dispatch the BESS correctly for peak-shaving purposes.
The control can be described by (1) and (2):

$$P_{ems,ch,t} = \begin{cases} P_G^{max} - P_{EV,t}, & P_{EV,t} < P_G^{max} \\ 0, & SoC_{b,t} > 90\% \end{cases} \quad (1)$$

$$P_{ems,dis,t} = \begin{cases} P_{EV,t} - P_G^{max}, & P_{EV,t} \geq P_G^{max} \\ 0, & SoC_{b,t} < 5\% \end{cases} \quad (2)$$

Charging of the BESS occurs when the demand of the station $P_{EV,t}$ is smaller than the maximum grid-tie capacity P_G^{max}. On the contrary, discharging occurs when the FCS demand is larger than the grid-tie capacity. Both are only valid when the BESS is within its SOC constraints given by (3):

$$5\% \leq SoC_{b,t} \leq 90\% \quad (3)$$

If this is not the case the BESS will go into idle mode. For each condition a BESS mode signal B_{mode} is generated. Furthermore, the EMS determines the grid-tie demand $P_{G,t}$ during both periods using (4).

$$P_{G,t} = \begin{cases} P_{EV,t} + P_{b,ch,t}, & P_{EV,t} < P_G^{\max} \\ P_G^{\max}, & P_{EV,t} \geq P_G^{\max} \end{cases} \quad (4)$$

C. Battery Energy Storage System

The BESS model describes the BESS at a higher level of abstraction through analytical equations and requires only the SOC, charging/discharging power, efficiency and energy capacity to model it's performance [16].
According to the battery mode signal received from the EMS, the battery either goes into charge, discharge or idle mode. In both charge and discharge mode, the power constraints are applied to the EMS power signal, the inverter efficiency determined and energy added or removed from the previous BESS energy content $E_{b,t-1}$. In idle mode the BESS does not charge nor discharge any energy. Equation (5) describes this charging, discharging and idling procedure.

$$E_{b,t} = \begin{cases} E_{b,t-1} + \dfrac{P_{b,ch,t}}{60} \cdot \eta\left(P_{b,ch,t}\right), & B_{mode} = \text{Ch.} \\ E_{b,t-1} - \dfrac{P_{b,dis,t}}{60} \cdot \dfrac{1}{\eta\left(P_{b,dis,t}\right)}, & B_{mode} = \text{Dis.} \\ E_{b,t-1}, & B_{mode} = \text{Idle} \end{cases} \quad (5)$$

To ensure the BESS model (dis)charges within it's power and energy capabilities, the following energy constraint (6) and power constraint (7) are applied.

$$0 \leq E_{b,t} \leq E_b^{cap} \tag{6}$$

$$0 \leq P_{b,ch,t}, P_{b,dis,t} \leq P_b^{max} \tag{7}$$

Furthermore, the (dis)charge power of a BESS is not fully constant over the full range of SOC, at low (around 15%) and high (around 80%) levels the power linearly decreases according to (8) and (9) [17].

$$P_{b,ch,t} \leq \frac{P_b^{max}}{1 - S_{b,ch}} \left(\frac{E_{b,t}}{E_b^{max}} - 1 \right) \tag{8}$$

$$P_{b,dis,t} \leq \frac{P_b^{max}}{S_{b,dis}} \left(\frac{E_{b,t}}{E_b^{max}} \right) \tag{9}$$

To model the BESS inverter, a 3 segment piece-wise linear approximation of an inverter curve model from [18] is implemented and described by (10):

$$\eta = \begin{cases} 8.8 \cdot P_{b,t} + 0.05, & P_{b,t} \leq 0.1\text{pu} \\ 0.93 + (0.1 \cdot (P_{b,t} - 0.1)), & P_{b,t} \leq 0.5\text{pu} \\ 0.97, & P_{b,t} \leq 1\text{pu} \end{cases} \tag{10}$$

Lastly, at the end of each step the SOC is determined by (11):

$$SoC_{b,t} = \frac{E_{b,t}}{E_b^{cap}} \cdot 100\% \tag{11}$$

D. BESS Lifetime

The lifetime module estimates the expected lifetime of the BESS using its SOC profile. This module uses the post-processing lifetime model proposed in [13] to determine the capacity fade being induced by the cycle and calendar degradation factors on LFP/C batteries. By knowing the degradation for a certain SOC profile, one can estimate the time it takes for the battery to reach it's EOL criterion of 80% [19]. This is taking the assumption that the battery will repeat this SOC profile during the entirety of its lifetime.
Using a slightly modified version of the rain-flow cycle counting algorithm found in [19], the cycles are counted based on a discrete n segments of DOD ranges and average SOC. Where these discrete segments are used in order to obtain computational simplicity. However, to preserve model accuracy a minimum of 20 discrete segments are selected [20].

E. Charging Delay

The QoS module determines the performance of a BESS assisted FCS design in terms of charging delays. Charging delays would be experienced at times when the power delivered from both the grid-tie and BESS cannot meet the EV demand, and thus resulting in a longer charging session due to the reduced charging speeds. The module starts by identifying power mismatch moments, these are periods where a power differences exist between the EV demand $P_{EV,t}$ and the FCS power capability $(P_{G,t} + P_{b,dis,t})$. When a power mismatch moment is identified ($\Delta P_t > 0$), then the extra time Δt_d it takes to charge the missed energy ΔE_t at the available FCS power is determined. This is then summed up until a mismatch period ends ($\Delta P_t \leq 0$). When a mismatch period ends, an estimate of the total charging delay ($T_{delay,t}$) for the ending power mismatch period is obtained by equally dividing the summed Δt_d over the number of charging EVs $N_{EV,t}$. Fig. 2 displays a flow-chart for a simulation step of this module.

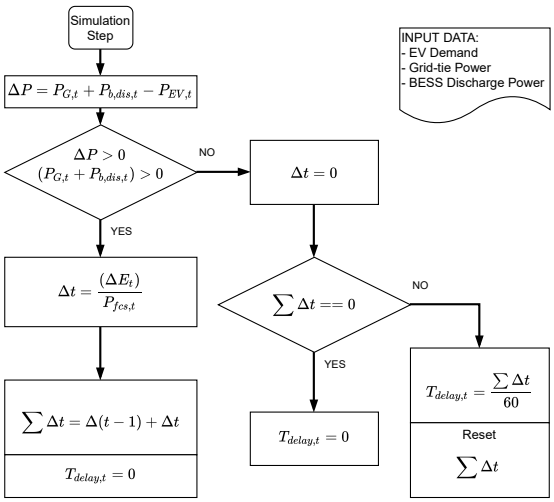

Fig. 2: Quality of Service implementation flowchart

III. Multi-objective problem formulation

A. FCS Design Problem

The optimization framework proposed in this paper considers two contradicting design objectives, the associated DCM costs and the station's performance. The DCM cost component consists of the annual demand charges and the annual BESS investments required to perform the peak-shaving. The performance is measured in the charging delays that customers experience when there is not sufficient power capacity available from both the grid-tie and BESS to meet the EV charging demand. Using a station's demand profile and the 3 design parameters, maximum grid-tie power P_G^{max}, BESS capacity $E_b^{\max}$ and BESS power rating $P_b^{\max}$ both objectives can be evaluated with the FCS model proposed in Section II. Moreover, another assumption made is that the BESS will be in service for the duration of its expected lifetime. This way the initial BESS investments are annualized to be included in the annual DCM cost. Furthermore, to properly asses a stations performance, two KPIs are derived from the charging delays $T_{delay,t}$, the maximum charging delay and the increase in station utilization. The maximum charging delay is the maximum extra time an EV customer might experience to complete it's charging session.
Increase in utilization is here defined as the percentage increase in the total amount of time the station is being occupied due to additional charging time. This KPI gives an indication on how frequent delays occur, and thus affecting

the owner's sales potential due to increased station occupation.

B. Objective functions & Design Constraints

The objective function (12) represents the DCM cost function, which describes the BESS related investments associated to the DCM design and the reduced demand charges. The annual BESS costs compromises of BESS project costs annualized by the expected BESS lifetime L_{exp} in years. An additional over-sizing factor β_{cap}= 1.2 and β_{pow}= 1.07 are included to take into consideration the capacity and power fade due to degradation [21]. Furthermore, the monthly demand charges C^{dem} are annualized using the factor $\alpha = 1/12$.
Due to the subtle differences in dependencies between the maximum charging delays and the utilization time increase, the performance objective is further separated into a two separate objective functions (13) and (14), to discard solutions with low maximum delays, but frequent delays.
Apart from the constraints included inside the FCS model, a set of design constraints are applied to restrict our search during the optimization using previous knowledge and BESS chemistry constraints obtained from literature. Constraint (15) represents the power to energy (P/E) ratio constraint related to the LFP/C chemistry considered [11], (16) restricts the optimization from selecting solutions outside the stations relevant power demand boundaries [10] and (17) restricts the optimization from selecting solutions with maximum delays longer than 8 minutes since most FCS customers are likely not willing to wait longer than that [6].

$$\min_x f_1(x) = C^{DCM} = \frac{C^{bess} E_b^{\max} \beta_{cap} + C^{conv} P_b^{\max} \beta_{pow}}{L_{exp}} + \frac{C^{dem} P_G^{\max}}{\alpha} \tag{12}$$

$$\min_x f_2(x) = T_{\max} = \max(T_{delay,t}) \tag{13}$$

$$\min_x f_3(x) = T_{freq} = \frac{\sum T_{delay,t}}{T_{charging}} \cdot 100\% \tag{14}$$

$$s.t.\ X^{\min} P_b^{max} \leq E_b^{cap} \leq X^{\max} P_b^{max} \tag{15}$$

$$P_{fcs-avg} \leq P_G^{max} + P_b^{max} \leq P_{fcs-max} \tag{16}$$

$$T_{max} \leq 8 \tag{17}$$

C. Sizing Framework

The framework shown in Fig. 3 consist of the FCS model, using a FCS worst case demand profile, and the MOO optimization model, using NSGA-II implemented in Pymoo [22]. In order to obtain a FCSs and BESSs design that can endure usage during worst case scenarios, a worst case demand profile (for the period around Christmas holidays) was selected as input for the FCS model [23]. The demand profile comprises of two worst 24-hour periods. One with the worst peak demand, to ensure the power requirements and one with the worst energy density, to ensure the BESS energy requirements [17]. Furthermore, the charging delay and expected BESS lifetime

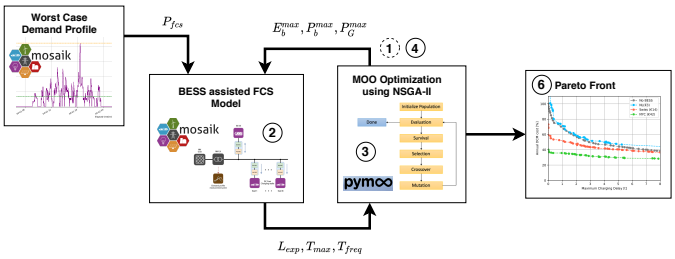

Fig. 3: A schematic overview of the proposed design optimization framework

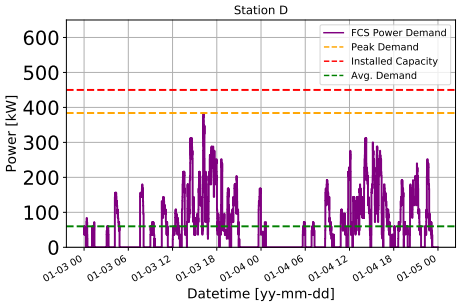

Fig. 4: Worst case charging demand profile for the FCS

is assessed separately for each period, where the worst from the two periods is selected. For reasonable computational time inside the Pymoo implementation, the population size is set to a fixed size of n_{pop}= 50 and the termination criterion is defined by a design space tolerance of 1%. Which should be sufficient to give an accurate indication of the sizing considering the power ranges in FCS applications.
The framework can be described in the following six steps: step 1, an initial population consisting of the 3 design parameters (P_G^{max}, $P_b^{\max}$ and $E_b^{\max}$) are generated using the NSGA-II properties, step 2, the FCS model is ran using this population and their corresponding performance parameters ($L_{\exp}$, $T_{\max}$ and T_{freq}) are extracted, step 3, using all six variables the objective functions are evaluated, step 4, using NSGA-II a new parent population is extracted for the next generation, step 5, step 2-4 is repeated until the termination criterion is met, step 6, once this criterion is met, an estimate of the Pareto front is considered to be found.
Using the objective space and design space data, an FCS host can use higher level information to select the optimal station design. Such higher level information can be for example investment budgets or location specific QoS requirements.

IV. Case Description

In this paper an FCS with the following characteristics is being used as a case study. The station has 4 charging stalls with a total installed capacity of 450 kW, a peak demand of 384 kW and an average demand of 60 kW. A worst case demand profile extracted from the energy measurement data for this station is presented in Fig. 4.

TABLE I: List of the study cases for the optimization

Study Case	Description	BESS	Demand Tariffs
Case 1:	DCM without BESS	Excl.	
Case 2:	BESS assisted DCM	Incl. C^{bess}=€490/kWh [24] C^{conv}=€110/kW [25] 1/8 <P/E ratio < 1 [26]	NL = €2.7/kW [27] Swiss = €14.4/kW [10] NYC = €42.3/kW [4]

Furthermore, to serve as a benchmark and asses the effectiveness of BESS solutions, both DCM with and without BESS are considered. Additionally, to asses the effects of different demand tariffs on our optimization, it is performed for several demand tariff regions. These are done for the Netherlands (NL), Switzerland (Swiss) and New York City (NYC). Table I presents these cases along with the cost/technology parameters used in the optimizations.

It should be noted that, when assessing the objective space the annual DCM cost is given as a percentage of the stations annual demand charges without DCM. Similarly, the grid-tie size and BESS power capability is given in per units. Both are based on the station's peak power demand as the base value.

V. Numerical Results

A. Optimal design in different demand tariffs

These results are intended to show how the optimum sizing is influenced by different demand tariffs. This illustrates how the objective and design space moves for a certain station demand employed in different demand tariff regions. Fig. 5 displays how the objective space move in terms of DCM cost and maximum charging delays and Fig. 6, 7, 8, and 9 shows how the design parameters move with respect to maximum charging delays for the different regions.

Fig. 5 shows that a significant DCM cost reduction can be obtained in high demand tariff regions relative to applying only power balancing. However, this is not the case for regions with low demand tariffs such as for NL, where this performed worse than power balancing in terms of costs. In contrast, for Swiss and NYC, DCM reductions between 40-60% and 60-70%, respectively can be obtained depending on the delays. Furthermore, observing how the grid-tie moves in Fig. 6 with respect to the different regions, a dramatic 80% of grid-tie reduction can be achieved in NYC.

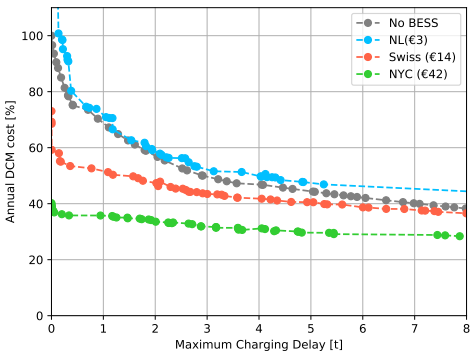

Fig. 5: DCM cost vs max. charging delay [min]

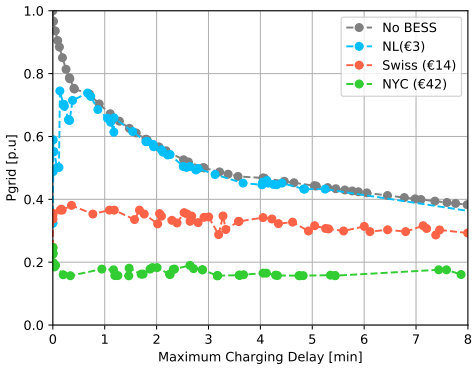

Fig. 6: Grid-tie size [pu] vs max. charging delay [min]

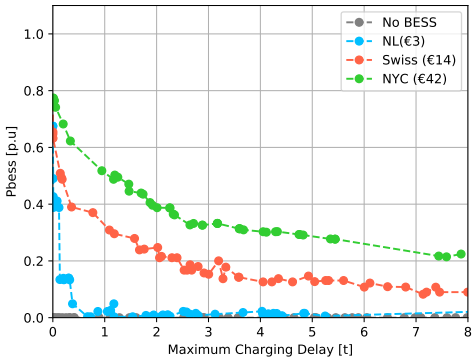

Fig. 7: BESS power rating [pu] vs max. charging delay [min]

Nevertheless, as longer delays are permitted, the differences in performance between power balance only and the other two regions diminishes. Where for 8 minute delays, in Swiss the station performs equally and in NYC with a difference of only 10% in terms of cost. In terms of grid-tie, a difference of 10% and 20% can be obtained with 8 minute delays, respectively. Regarding the BESS sizing shown in Fig. 7 and 8, except for some expensive solutions around zero delays, in the NL case the BESS is excluded for most of the solutions and the power balance curve is given as the optimal solution. For the NYC case, the BESS sizing behaves similarly to the Swiss case in terms of delays. However, it also evident that high demand tariffs directly impact the feasible BESS capacities, a 3x difference in demand tariff between Swiss and NYC is reflected in the BESS capacity increase. Furthermore, the same is observed between the two power parameters, the additional 20% decrease in the grid-tie can found in the increase of the BESS power capabilities.

Fig. 9 illustrates how the different demand tariffs influence the optimal BESS PE ratios. For the NL case, except for some expensive outliers, the optimal solutions concentrate around the origin, due to either suggesting a really small BESS or none at all. For the Swiss case, the P/E ratio (highlighted in

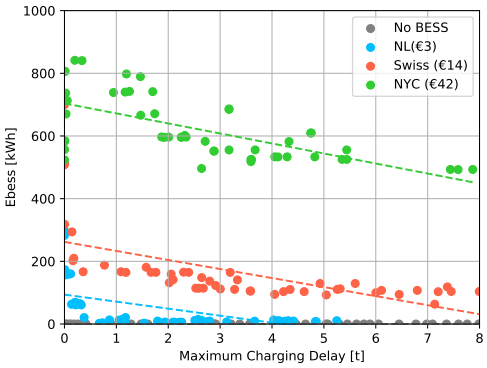

Fig. 8: BESS energy rating [kWh] vs max. charging delay [min]

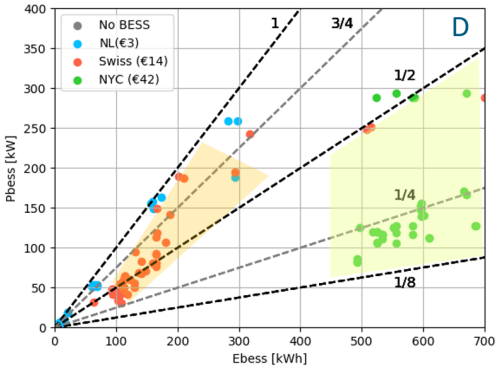

Fig. 9: BESS power [kW] vs energy rating [kWh]

orange) concentrates between 1 and 1/2. The NYC case, larger BESS capacities are introduced, making the optimal solutions (highlighted in green) concentrate between 1/2 and 1/8. Due to the almost direct correlation between the demand tariffs and BESS capacities, FCSs located in regions with high demand tariffs optimally should posses larger capacities, and thus lower P/E ratios than for stations in regions with mid range demand tariffs.

B. Performance simulations

In this section the performance of the FCS is assessed by selecting a number of optimally sized 2 minute delay solutions (rounded to the nearest 5 kW/kWh) and simulate this on an entire week demand wherein the peak demand occurs. The results include the charging delays, the SOC profile of the BESS and the power flows.

The simulation results of an optimal design without BESS is shown in Fig. 10 and a BESS included solution in Fig. 11. Both are simulated for for the Swiss demand tariff case. When comparing these results, it becomes clear that in the BESS included design the BESS power and grid-tie combined are slightly larger than the grid-tie size in the non-BESS solution. This small difference in rating and maximum delay are due to the fact that the BESS reaches below it's 15% SOC threshold,

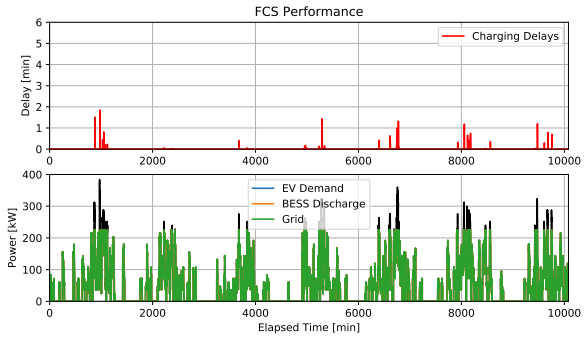

Fig. 10: Power flow and charging delays of a 2 min delay FCS in Swiss without BESS. P_G = 225kW, DCM Cost = 38,880 €/year (-41.4%)

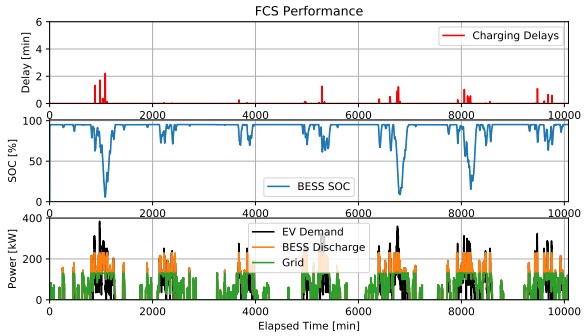

Fig. 11: Power flow and charging delays of a 2 min delay FCS with BESS in Swiss. $E_b^{\max}$= 135kWh, $P_b^{\max}$ = 100kW, P_G^{max} = 130kW, $L_{\exp}$ = 11 years, DCM Cost = 30,750 €/year (-53.7%)

causing the power capabilities of the to BESS decreases, and thus causing additional power mismatch. This is also visible in the way the delay peaks differ during this period. Nevertheless, the BESS included solution will result in a 10% lower DCM cost compared to the DCM solution without BESS with a total of 53% reduction in demand charges.

Fig. 12 shows the results of a 2-minute optimal solution the FCS located in NYC. These results show that even with different design ratios, the optimal charging delay performances do not differ much per region. However, as observed from the optimizations, the P/E ratios are reduced, and thus larger BESS capacities are introduced causing longer cycles.

This reduces the opportunity to dispatch the BESS for other ancillary services. However, these longer cycle periods are more shallow and the high SOC idling periods are shorter, resulting in improved BESS lifetimes.

VI. Conclusion

This paper presented the methodology and framework, for multi-objective optimization for BESS design in FCSs. The results presented shows that the BESS capability curves

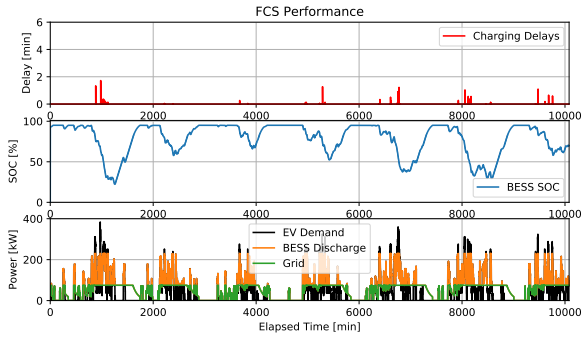

Fig. 12: Power flow and charging delays of a 2 min delay FCS with BESS in NYC. $E_b^{\max} = 600$kWh, $P_b^{\max} = 155$kW, $P_G^{max} = 75$kW - $L_{\exp} = 14$ years, DCM Cost $= 64,573$ €/year (-66.9%)

cause additional delays at times when the BESS is below its maximum power SOC threshold. Leading to the conclusion that power capability curves are essential when analysing delays caused by power differences, while they are not often taken into account in the literature. Furthermore, this paper investigated the impact of demand tariffs in the BESS sizing, considering the current prices in the cases of the Netherlands (€3/kW), Switzerland (€14/kW) and NYC (€42/kW). From the optimizations we can conclude that for the Netherlands nowadays the BESS costs are too high for profitability. This causes the optimization to roughly follow the power balance without BESS solutions. For Switzerland, between 40-60% cost reductions can be obtained depending on the accepted delays. For NYC a reduction between 60-70% is obtained, for this region the grid-tie is 10% smaller and P/E ratio of the BESS design is lower than in Switzerland. Leading to the conclusion that high demand tariff regions require lower P/E ratios as optimal design. A 2-minute delay optimal solution was simulated against a weekly demand and the effectiveness is confirmed. Remarkable is that optimal designs in different tariffs obtain the same delay performance but with different BESS performances in terms of power flows and cycling depth/lengths. Overall, this paper showed that BESS can benefit the business case of FCS in high demand tariff regions, if the correct sizing ratios between the grid-tie and BESS are selected properly.

REFERENCES

[1] M. Neaimeh, S. D. Salisbury, G. A. Hill, P. T. Blythe, D. R. Scoffield, and J. E. Francfort, "Analysing the usage and evidencing the importance of fast chargers for the adoption of battery electric vehicles," *Energy Policy*, vol. 108, no. April, pp. 474–486, 2017.

[2] Cox Automotive Inc, "Overcoming Electric Vehicle Misconceptions is Crucial to Converting Consideration to Sales." [Online]. Available: https://www.coxautoinc.com/news/overcoming-electric-vehicle-misconceptions-is-crucial-to-converting-consideration-to-sales/

[3] Elaadnl, "Snel, sneller, snelst," 2019.

[4] NREL, "Identifying Potential Markets for Behind-the-Meter Battery Energy Storage: A Survey of U.S. Demand Charges," *NREL*, pp. 1–7, 2017.

[5] McKinsey & Company, S. Knupfer, and S. Sahdev, "How Battery Storage Can Help Charge the Electric-Vehicle Market," *McKinsey & Company*, no. February, pp. 1–8, 2018.

[6] T. S. Bryden, G. Hilton, B. Dimitrov, C. Ponce De León, and A. Cruden, "Rating a Stationary Energy Storage System Within a Fast Electric Vehicle Charging Station Considering User Waiting Times," *IEEE Transactions on Transportation Electrification*, vol. 5, no. 4, pp. 879–889, 2019.

[7] L. Richard and M. Petit, "Fast charging station with battery storage system for EV: Grid services and battery degradation," *2018 IEEE International Energy Conference, ENERGYCON 2018*, pp. 1–6, 2018.

[8] M. Gjelaj, N. B. Arias, C. Traeholt, and S. Hashemi, "Multifunctional applications of batteries within fast-charging stations based on EV demand-prediction of the users' behaviour," *The Journal of Engineering*, vol. 2019, no. 18, pp. 4869–4873, 2019.

[9] V. Salapic, M. Grzanic, and T. Capuder, "Optimal sizing of battery storage units integrated into fast charging EV stations," *2018 IEEE International Energy Conference, ENERGYCON 2018*, pp. 1–6, 2018.

[10] Y. Ligen, H. Vrubel, and H. Girault, "Local energy storage and stochastic modeling for ultrafast charging stations," *Energies*, vol. 12, no. 10, 2019.

[11] M. Moradzadeh and M. M. A. Abdelaziz, "A New MILP Formulation for Renewables and Energy Storage Integration in Fast Charging Stations," *IEEE Transactions on Transportation Electrification*, vol. 6, no. 1, pp. 181–198, 2020.

[12] H. Tu, H. Feng, S. Srdic, and S. Lukic, "Extreme Fast Charging of Electric Vehicles: A Technology Overview," *IEEE Transactions on Transportation Electrification*, vol. 5, no. 4, pp. 861–878, 2019.

[13] D. I. Stroe, M. Swierczynski, A. I. Stroe, R. Teodorescu, R. Laerke, and P. C. Kjaer, "Degradation behaviour of Lithium-ion batteries based on field measured frequency regulation mission profile," *2015 IEEE Energy Conversion Congress and Exposition, ECCE 2015*, pp. 14–21, 2015.

[14] S. Schütte, S. Scherfke, and M. Sonnenschein, "mosaik - Smart Grid Simulation API," *Proceedings of SMARTGREENS 2012 - International Conference on Smart Grids and Green IT Systems*, no. 2, pp. 14–24, 2012.

[15] Fastned NL, "150+ kW fast chargers – Fastned support." [Online]. Available: https://support.fastned.nl/hc/en-gb/articles/115015420127-150-kW-fast-chargers

[16] S. You and C. N. Rasmussen, "Generic modelling framework for economic analysis of battery systems," *IET Conference Publications*, vol. 2011, no. 579 CP, p. 122, 2011.

[17] DNV GL, "Safety, operation and performance of grid-connected energy storage systems," Tech. Rep. December, 2015.

[18] Phase to Phase, "Vision Network Anlysis." [Online]. Available: https://phasetophase.nl/vision-network-analysis.html

[19] M. J. Alam and T. K. Saha, "Cycle-life degradation assessment of Battery Energy Storage Systems caused by solar PV variability," *IEEE Power and Energy Society General Meeting*, vol. 2016-Novem, pp. 1–5, 2016.

[20] B. Xu, J. Zhao, T. Zheng, E. Litvinov, and D. S. Kirschen, "Factoring the Cycle Aging Cost of Batteries Participating in Electricity Markets," *IEEE Transactions on Power Systems*, vol. 33, no. 2, pp. 2248–2259, 2018.

[21] D. Ioan, "Lifetime Models for Lithium Ion Batteries used in Virtual Power Plants Daniel-Ioan Stroe," Ph.D. dissertation, Aalborg University, 2014.

[22] J. Blank and K. Deb, "Pymoo: Multi-Objective Optimization in Python," *IEEE Access*, vol. 8, pp. 89 497–89 509, 2020.

[23] T. S. Bryden, G. Hilton, A. Cruden, and T. Holton, "Electric vehicle fast charging station usage and power requirements," *Energy*, vol. 152, pp. 322–332, 2018. [Online]. Available: https://doi.org/10.1016/j.energy.2018.03.149

[24] International Renewable Energy Agency (IRENA), *Electricity storage and renewables: Costs and markets to 2030*, 2017, no. October.

[25] NREL, "2018 U . S . Utility-Scale Photovoltaics- Plus-Energy Storage System Costs Benchmark," *National Renewable Energy Laboratory*, no. November, p. 32, 2018.

[26] U.S. Department of Energy, "Energy storage for power systems applications: a regional assessment for the northwest power pool (NWPP)," no. April, p. 104, 2010.

[27] Liander, "Tarieven voor aansluiting en transport gas," pp. 2–3, 2020. [Online]. Available: www.liander.nl/voorwaardenkleinverbruik